Locally Welded Silver Nano-Network Transparent Electrodes with High Operational Stability by a Simple Alcohol-Based Chemical Approach

*Haifei Lu, Di Zhang, Jiaqi Cheng, Jian Liu, Jian Mao, and Wallace C. H. Choy**

As an indispensable aspect of emerging flexible optoelectronics, flexible transparent electrodes, especially those comprised of metal nanowires, have attracted great attentions recently. Welding the nanowire junctions is an effective strategy for reducing the sheet resistance and improving the operational stability of flexible nanowire electrode in practical applications. Herein, a simple alcohol-based solution approach is proposed to weld crossed silver nanowires by chemically growing silver "solder" at the junctions of the nanowires, forming transparent silver nano-network electrodes with improved electrical conductivity and operational stability. Remarkably, silver nano-networks can be rapidly formed by this simple approach under ambient condition and room temperature, requiring no assistance from heat, light, electrical current, or mechanical pressure. Furthermore, our results show that the nano-network electrode formed from large diameter nanowires offers a better operational stability, whose trend is opposite to that of the untreated electrodes. To demonstrate the potential application of the highly stable silver nano-network from large diameter nanowires, organic solar cells fabricated on the nano-network electrode incorporated with silicon dioxide nanoparticles achieve comparable performance to the ITO control device. Consequently, strategy demonstrated in this work can contribute to low-cost and highly stable transparent electrodes in emerging flexible optoelectronics.

1. Introduction

Owing to the existing concerns regarding the rare indium element and the brittle property of tin-doped indium oxide (ITO), increasing efforts have been made to develop alternative transparent electrodes for the growing optoelectronic applications during recent years.[1–6] Silver nanowires (Ag NWs), being one of the most promising alternatives as well as candidates for next-generation flexible transparent electrodes, have received great amount of attention.[7–12] In order to achieve silver nanowire-based transparent electrodes, Mayer rod, doctor blade, vacuum filtration, spray gun, and spin-coater are generally adopted for coating the silver nanowires on specific substrate.[13–17] However, the as-formed silver nanowire electrode would exhibit poor conductive and stability performances because of their large contact resistance.[18] The coating of additional material on silver nanowire film, such as poly(3,4-ethylenedioxythiophene):polystyrene sulfonate (PEDOT:PSS), TiO_2, ZnO, graphene, graphene oxide, carbon nanotube, etc., for welding the silver nanowires has been recently reported,[19–28] which will however alter the work function of the nanowire electrodes. Previous welding approaches without introducing different material with the nanowires would involve the assistance of heat, electrical current, mechanical pressure, and light,[13,18,29–35] which will have concerns to meet the broad requirements in the emerging flexible optoelectronic field. Therefore, forming highly stable and conductive silver nanowire transparent electrode adaptable for versatile electrode applications (both anode and cathode) through simple, low-cost, and time-saving approach at room temperature and ambient condition would be highly desirable.

The application of silver nanowires in organic solar cell (OSC), with its efficiency rapidly improved recently,[36–46] would greatly benefit the realization of all solution processed, low-cost, and flexible device. However, in previous reports, thin silver nanowires with diameter smaller than 30 nm have been selected and utilized for bottom electrodes of OSCs,[47–52] since nanowire film with relatively small surface roughness can be easily flattened by traditional interfacial materials. Although silver nanowires with larger diameter are much more thermally and chemically stable, fewer studies have focused on their usage (e.g. 100 nm in diameter), as the increased surface roughness of the electrodes can lead to leakage current and deteriorated performance for thin film optoelectronic devices if not properly addressed. Suppressing the surface roughness of nanowire electrodes with large diameter for practical optoelectronic device applications is still a challenging issue. At present, the methods reported for addressing the issue still involve mechanical pressing of silver nanowires or transferring silver nanowires into polymer matrix.[53–55] Developing simple and

Dr. H. Lu, Dr. D. Zhang, J. Cheng, Dr. J. Liu, J. Mao, Prof. W. C. H. Choy
Department of Electrical and Electronic Engineering
The University of Hong Kong
Pokfulam Road, Hong Kong SAR, P. R. China
E-mail: chchoy@eee.hku.hk

DOI: 10.1002/adfm.201501004

applicable approach for achieving highly stable nanowire transparent electrode and reducing the surface roughness of silver nanowires is therefore exceedingly necessary and highly relevant to practical applications.

In this paper, we propose and demonstrate a simple alcohol-based solution approach for chemically welding silver nanowires together to form silver nano-network. It involves the wetting of silver nanowire film by precursor, followed by chemical reduction of silver ions particularly at the cross regions of the nanowires during spin-coating or gas-blowing, due to the capillary force of liquid. The localized chemical reaction deposits the reduced silver atoms at the cross of silver nanowires for forming silver solder. With the presence of silver crystalline solder, the operational stabilities of the highly conductive silver nano-network under continuous external electrical bias are remarkably improved. Moreover, our experimental results show that the nano-network electrode from large diameter nanowire offers better operational stability, exhibiting opposite trend to that of the untreated nanowire electrodes. To demonstrate the highly stable silver nano-network in OSC application, insulating silicon dioxide (SiO_2) nanoparticles (NPs) have been used to form Ag nano-network:SiO_2 NPs composite electrode with reduced surface roughness. OSCs fabricated on our electrodes have been studied and the power conversion efficiency (PCE) is comparable to that of the ITO-based control device. The high PCE of OSCs using the composite electrode is a distinctive improvement over that of nano-network devices without SiO_2 NP flattening, which exhibits shorting by the direct contact between the bottom and top electrodes. Consequently, conductive silver nano-network forming from the simple strategy with considerably improved operation stability has been proposed and demonstrated in OSC application, which will contribute to the fast developing evolution of flexible optoelectronics.

2. Results and Discussion

For chemical formation of silver "solder" at the junction of silver nanowires, silver nitrate and ascorbic acid were selected as the silver salt and reduction reagent respectively, which were dissolved in ethanol for demonstration. It should be noted that the reaction between silver nitrate and ascorbic acid in ethanol is rapid and vigorous even at room temperature. Large amount of silver nanoparticles will form once the two reagent solutions were mixed, and the size of nanoparticles would increase quickly as indicated by the color change of solution. Hence, it is difficult to employ a direct mixture of the two reagent solutions as the precursor for our proposed chemical treatment. Suitable control on the rapid reaction would be necessary for the followed localized chemical welding process.

Here, we add a proper amount of nitric acid to silver nitrate solution before mixing with the ascorbic acid solution. It is found that an acidic environment with a PH value of about 3 can efficiently prohibit the reaction between silver nitrate and ascorbic acid. The precursor solution will keep clear after long-time incubation at room temperature. However, the redox reaction will be quickly activated when the mixture solution is exposed to silver nanoparticles or silver nanowires, which allows us to control the reaction merely at the junction of silver nanowires. Briefly, after the wetting of the silver nanowire film by the precursor, the redox reaction and silver atoms deposition will quickly initiate at the contact region between silver nanowires, which has relatively high chemical potential because of the creation of concave-type surface.[56,57] Either spin-coating or dry-blowing approach would help to remove the superfluous precursor from the surface, while leaving small amount of precursors trapped at the junction regions contributed from the capillary force. Consequently, solid silver solders at the crosses of silver nanowires will form. It should be noted that other alcohols, such as methanol, isopropyl alcohol, butanol, etc., and the mixture of alcohol–water can also be used for our proposed chemical reaction, which will provide different solvent options in practical applications depending on the wetting property of the surface. In addition, some of the alcohols, such as ethanol, isopropyl alcohol, and methanol, have lower boiling points than water, which allow them to dry quickly. Thus, the effect and damage of the underneath water-sensitive material can be minimized as compared to the aqueous approach. Detailed description on the experiment can be found in the Experimental Section.

Figure 1b,d,f shows the SEM images of silver nano-network formed from different diameters of nanowires (about 100, 60, and 20 nm in average, respectively) after our proposed chemical treatment. Solid solders can be clearly distinguished from the crosses of the treated silver nanowires, as compared to the corresponding control samples without chemical treatment as shown in Figure 1a,c,e. Transmission electron microscope (TEM) and energy-dispersive spectrometer (EDS) have been also adopted for the characterization of the solder at the cross region of silver nanowires. **Figure 2**b,c shows the EDS spectra collected from silver nanowire and solder, respectively, as the red circles indicated in Figure 2a. The good consistency of the two spectra indicates that the solder has the same material as silver nanowire. In addition, the microarea electron diffraction (MAED) pattern in the inset of Figure 2a further proves that the chemically formed solder is comprised of highly crystalline silver.

Regarding the optical transparency, owing to the efficient confinement of chemical reaction at the junction, the amount of the introduced silver material is quite small, and the loss of the optical transmission of silver nanowire electrodes after chemical treatment can be nearly negligible. The transmission of 100 nm diameter Ag nanowire electrode is shown in Figure 2d. The trend of the transmission of 20 and 60 nm diameter Ag nanowire electrodes is similar to that of 100 nm diameter Ag nanowire electrode as shown in Figure S1 in the Supplementary Information. For nanowires with large diameter (such as 100 nm), the contact area between nanowires without any treatment would be much smaller than the diameter due to their stiffness feature, which will significantly reduce the electrical conductivity of the electrode. Through our approach, the crystalline silver solder formed at the cross would greatly increase the contact area between silver nanowires and thus reduce their contact resistance. Therefore, the sheet resistance of transparent electrodes from 100 nm silver nanowires has been greatly reduced to 20.5 Ω sq^{-1}, which is five orders smaller than the one before chemical treatment (3.5 million Ω sq^{-1}). Similar trend has also been observed for the electrode formed from small-diameter nanowires, albeit the improvement is smaller. This can be due to the natural property of small nanowires, which

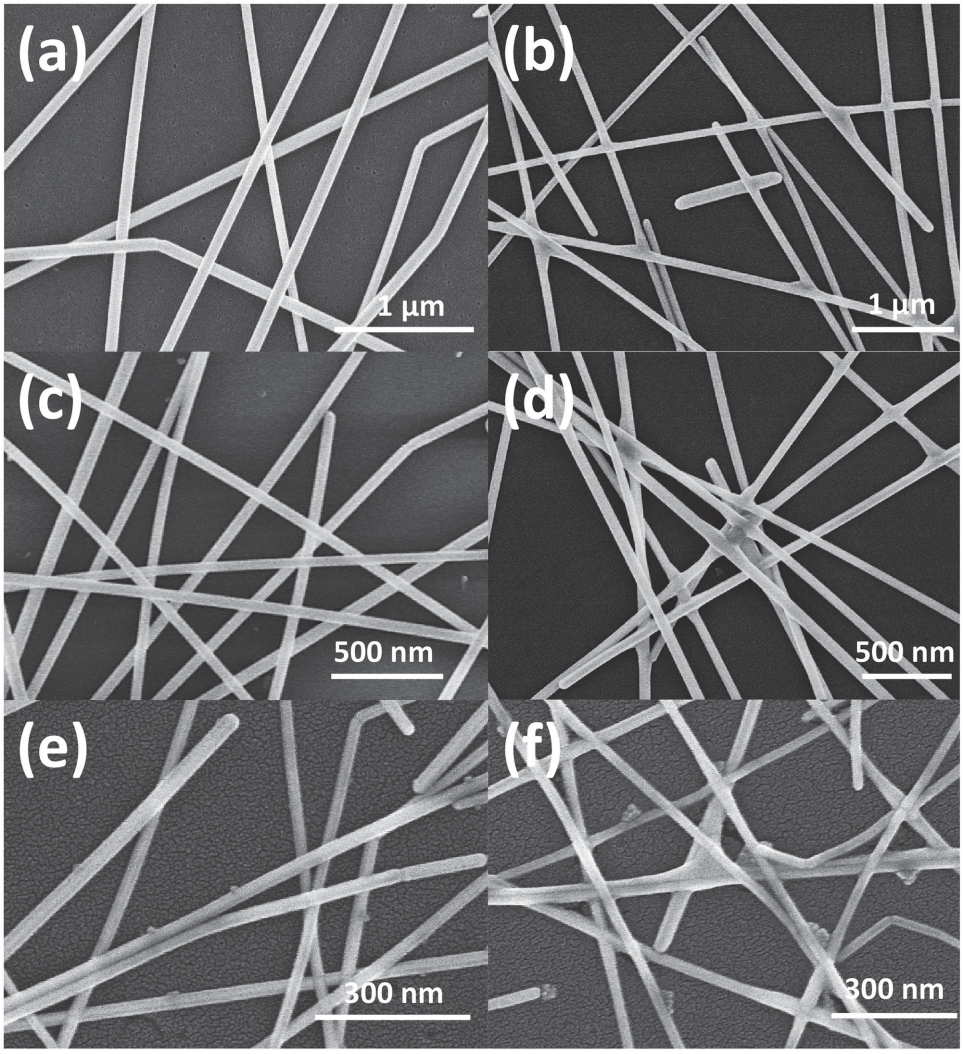

Figure 1. SEM images of transparent electrodes fabricated from a,b) 100, c,d) 60, and e,f) 20 nm silver nanowires before and after chemical treatment, respectively.

are relatively soft, and their contact area could be comparable to the nanowire diameter. Even though the contact area of silver nanowires is greatly enlarged after the growth of silver solder, according to Pouillet's law, the small diameter of silver nanowires will restrict the improvement of conductivity.

Besides optical transparency and electrical conductivity, it is well known that the operational stability of transparent electrodes under continuous external electrical bias is critical to their practical applications in electronic and optoelectronic devices. Remarkably, the presence of the chemically bonded silver solder will also greatly improve the electrical stability of silver nanowire electrodes under continuous external electrical bias. As shown in **Figure 3**, we plotted the resistance variations of transparent electrodes made from silver nanowires of different diameters with and without chemical treatment under a constant external voltage bias (details are described in the Experimental Section). To acquire a fair comparison, the electrodes made from silver nanowires of three different diameters after the chemical treatment were adjusted to have the same sheet resistance. From the resistance variations over time, it can clearly be seen that for silver nanowires without the chemical treatment, the electrode either has too large resistance (for 100 nm diameter nanowire) or broken down within merely ≈1 h of constant voltage bias for the cases of other diameters as shown by the open symbol lines in Figure 3. Interestingly, the electrical stabilities of silver nanowire electrodes of all nanowire diameters are dramatically improved by our chemical treatment as shown by the filled symbol lines. It should be noted that negligible optical transmission variation of the chemically treated nanowire electrodes has been observed after long period of applied external voltage bias.

More importantly, the stability of nanowire electrodes (untreated and chemically treated) showed a strikingly different trend with increasing nanowire diameters. For the untreated electrodes, smaller-sized nanowires demonstrate relatively better stability: for 20 nm nanowires, the relatively low resistance of the untreated electrode lasted for ≈70 min before broken-down; while for 60 nm nanowires, the electrode spiked rapidly within the first few minutes. Differently,

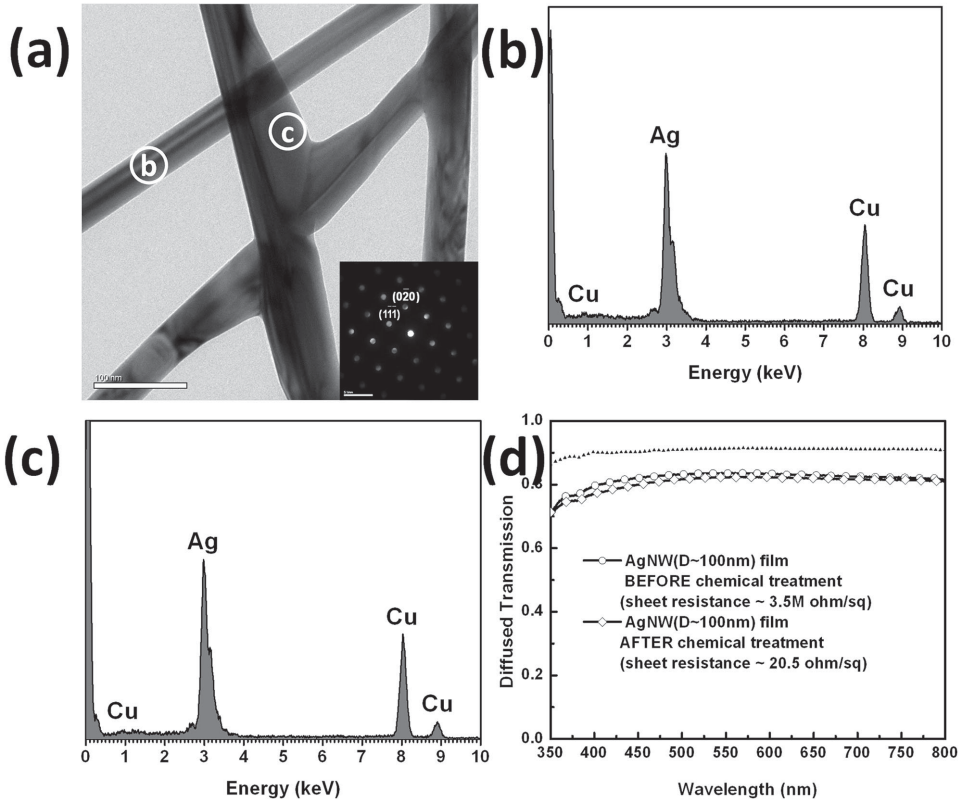

Figure 2. a) TEM image of crossed silver nanowires after chemical treatment. Parts (b,c) are the energy-dispersive spectroscopy (EDS) spectra collected from silver nanowire and solder, respectively, as indicated by circles ("b" and "c") in (a). Inset image is the microarea electron diffraction (MAED) pattern of the solder. d) Diffused transmission spectra of the transparent electrodes on glass substrates comprised by 100 nm silver nanowires before (black curve) and after (red curve) proposed chemical treatment. The sheet resistances of the silver nanowire electrode before and after chemical treatment are also provided. The black dash line is the transmission spectrum of bare glass substrate.

for electrodes treated with our chemical approach, much better stability was obtained in nanowires with larger diameters. For 20 nm chemically treated nanowires, the electrode failed after

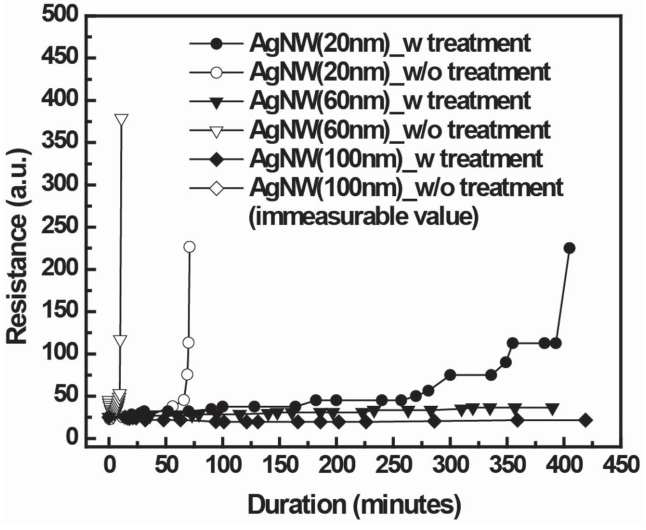

Figure 3. The resistance variation of different silver nanowire electrodes with and without chemical treatment under continuous external electrical bias.

400 min of voltage bias (resistance reaching ten times of the original value), while for the larger 60 nm nanowires, the resistance variation after 400 min voltage bias was reduced to 11 Ω. For the treated nanowires with the largest diameter (100 nm) in our experiment, we observed the best stability with almost unchanged electrical resistance: even after the whole measurement scope of 420 min, the maximal variation of electrode resistance was merely 4 Ω. That phenomenon can be attributed to two possible reasons. The first one is the variation of thermal tolerance from different diameter nanowires. Compared to the thick nanowires, relative low temperature will induce the burning-out of silver nanowires with small diameter, which will result in increasing the resistance of electrode. Another reason is related to the corrosion of silver nanowires by moisture, oxygen, or sulfur in the room ambient condition. The thin silver nanowire, having higher surface area to volume ratio, would be much easier to be attacked by the chemical species than the thick one, which will be even aggregated with the presence of electrical current.[58] Thus, silver nano-networks comprised by thick nanowires are more favorable for practical application, especially for high-power device, due to their electrically stable performance.

To demonstrate the potential application of silver nano-network electrode, especially the one from large diameter nanowires (e.g., 60 and 100 nm) with higher operational stability,

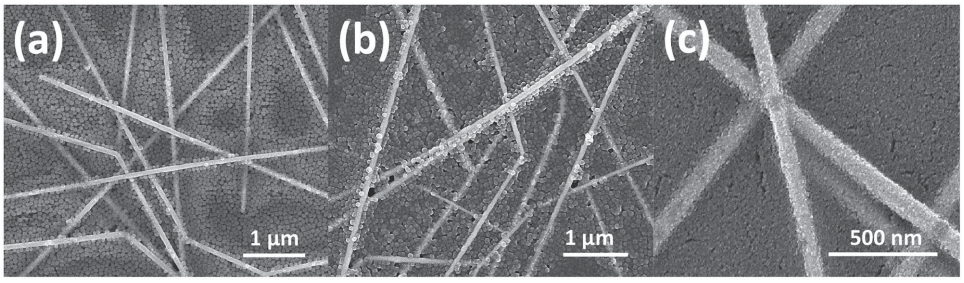

Figure 4. a) SEM images of silver nano-network electrode after SiO_2 NPs and b) further PEDOT:PSS coating. c) SEM image of Ag nano-network:TiO_2 electrode indicating the full coverage of TiO_2 NPs on the nanowire surface.

organic solar cells organic solar cells (OSCs) have been fabricated with the structure of Ag nano-network/PEDOT:PSS/poly(3-hexylthiophene):phenyl-C61-butyric acid methyl ester (P3HT:$PC_{61}BM$, 200 nm)/Ca (40 nm)/Al (100 nm). Control OSCs using commercial ITO as the anode are made for comparison. However, as shown in the inset of Figure 5a, both the OSCs fabricated from 60 and 100 nm silver nano-network only (as bottom electrodes) are short-circuited as indicated by the *J*–*V* characteristic curves passing through the zero points, due to the large surface roughness of bare silver nano-network. To overcome the surface roughness issue, we first adopted typical TiO_2 nanocrystals with diameter of 4 nm for flattening the silver nano-network. However, they will easily stick and cover on the entire surface of nanowires as shown in **Figure 4**c, which will affect the work function of silver nano-network electrode and charge extraction of the OSC device on the Ag nano-network:TiO_2 composite electrode. The optical transmission of Ag nano-network after TiO_2 NPs coating has been also greatly reduced as indicated in Figure S2 (Supporting Information). Consequently, all the parameters, including J_{sc}, V_{oc}, FF, and PCE, from the device using Ag nano-network (60 nm):TiO_2 composite electrode are significantly reduced compared to control device as listed in **Table 1**.

Meanwhile, we also use another typical nanoparticle of silicon dioxide (SiO_2) NPs with size of 50 nm, which are chemically stable, easily fabricated in different sizes, and have low refractive index for reducing the surface roughness of silver nano-network electrode. Despite the fact that SiO_2 NPs are insulating material, we find that the SiO_2 NPs efficiently fill the voids in silver nano-network. Interestingly, even though there are a small amount of SiO_2 NPs stay on the top surface of silver nano-network (see Figure 4a), a large portion of the upper surfaces of silver nanowires remain very clean as shown in Figure 4a, which will favor the good electrical contact between the silver nano-network and subsequently coated interfacial layer as will be further discussed later in device performances. In addition, the hydrophilic surface of SiO_2 NPs will greatly benefit the coating of various interfacial layers, such as PEDOT:PSS. By spin-coating PEDOT:PSS on the top of the electrode as a hole transport layer (the device properties will be described below), there is no considerable changes in the surface of Ag nano-network electrode as shown in Figure 4b. Besides, the roughness can be further smoothened by the PEDOT:PSS. Through adopting the proposed strategy, as the current density (*J*)–voltage (*V*) characteristics of OSCs and the device performances shown in **Figure 5**a and Table 1, respectively, the power conversion efficiency (PCE) of OSCs made from silver nano-network(60 nm):SiO_2 and nano-network(100 nm):SiO_2 reaches about 95% of the value from device using commercial ITO electrode. The achieved comparable fill factor (FF) proves that the introduction of SiO_2 NPs in silver nano-network electrodes does not bring notable negative effects on charge extraction and transportation properties in the device. Instead, the incorporated SiO_2 NPs effectively reduced the surface roughness of silver nano-network electrodes and thus minimized the current leakage through the direct contact between the bottom and top interfacial layers as indicated by the dark *J*–*V* curves in Figure 5b. The slight decrease of open-circuit voltage (V_{oc}) from two silver nano-network electrode devices can be attributed to the slightly difference of work function for chemically treated silver nano-network (–5.06 ± 0.02 eV) as compared to ITO after UVO treatment (–5.26 ± 0.02 eV). The slightly better short-circuit current (J_{sc}) of ITO device is due to the higher external quantum efficiency (EQE) of the OSC at the spectral region around 400 nm, as shown in Figure 5c. Although the optical transmission of silver nano-network electrode is slightly improved after SiO_2 coating, the optical transmission of the composite electrode is reduced after adding PEDOT layer. Conversely, the optical transmission of ITO substrate is improved after coating the PEDOT layer particularly at around 400 nm, as shown in Figure 5d, which contributed to the slightly better EQE of ITO-based OSCs as compared to Ag nano-network:SiO_2 NP-based OSCs.

Table 1. Summary of typical device performance of P3HT:$PC_{61}BM$ OSCs fabricated on the four transparent electrodes.

Device (P3HT:$PC_{61}BM$)	J_{sc} [mA cm^{-2}]	V_{oc} [V]	FF [%]	PCE [%]
ITO	9.62	0.62	62.1	3.704
Nano-network (60 nm):SiO_2	9.08	0.61	63.5	3.516
Nano-network (100 nm):SiO_2	9.16	0.61	62.6	3.498
Nano-network (60 nm):TiO_2	8.05	0.45	45.5	1.647

Besides P3HT:$PC_{61}BM$, we also demonstrate our composite electrode of Ag nano-network(100 nm):SiO_2 in OSC adopting small band-gap polymer of polythieno[3,4-*b*]-thiophene-*co*-benzodithiophene (PTB7). Details of device fabrication are described in the Experimental Section. The *J*–*V* characteristic and its performance are shown in Figure S3 (Supporting Information). A reasonably good PCE of 6.603% has been achieved for the device using our composite electrode, which further

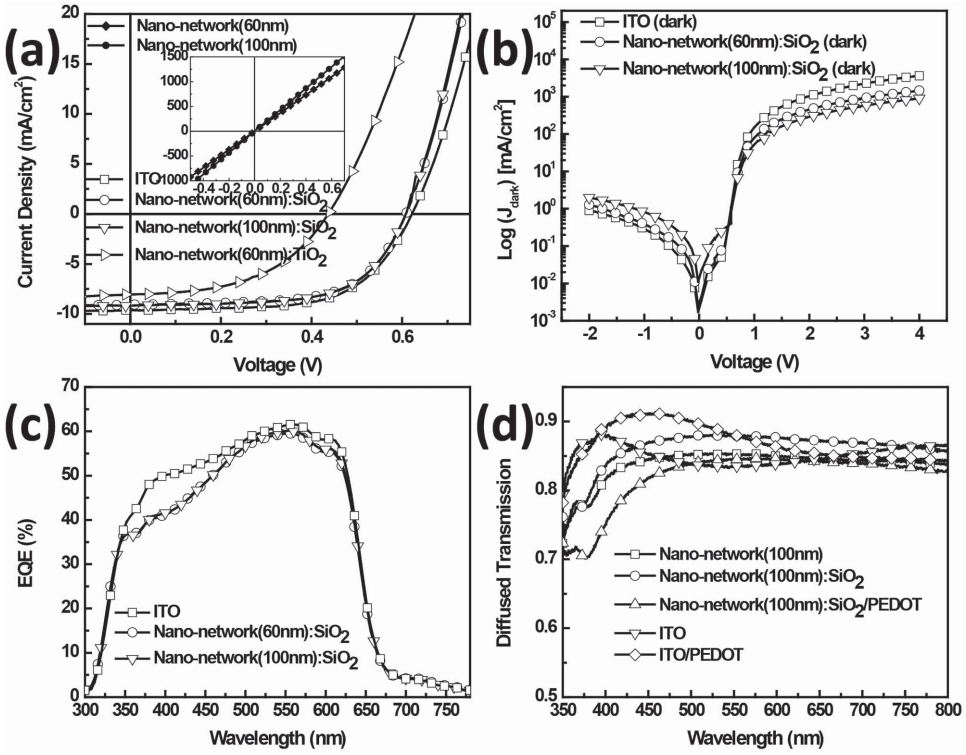

Figure 5. *J–V* characteristics of P3HT:$PC_{61}BM$ organic solar cells fabricated on different transparent electrodes under a) AM 1.5 G illumination and b) dark condition. Inset of (a) is the *J–V* characteristics of OSCs fabricated on bare silver nano-network electrodes without incorporation of SiO_2 NPs. Part (c) is the EQE results of the OSCs fabricated on ITO, silver nano-network(60 nm):SiO_2 and silver nano-network(100 nm):SiO_2 electrodes. Part (d) shows the diffused transmission spectra of one typical silver nano-network and ITO on glass after different materials coating.

proves our proposed strategy can enable silver nano-network comprised by large diameter nanowires, which have better operational stability performance for various organic optoelectronic applications.

3. Conclusion

In summary, a simple and alcohol-based solution approach has been proposed and demonstrated for chemically growing crystalline silver solder at the junction regions of silver nanowires for the formation of silver nano-network. By simply using spin-coating or dry-blowing, the precursor has been effectively confined at the junction region due to the capillary force of liquid. That will induce a localized chemical reaction and weld the silver nanowires together. Hence, the sheet resistances and operational stabilities of silver nano-network electrodes after proposed chemical treatment have been significantly improved, while less optical reduction of the electrodes has been observed. Moreover, our results show that the nano-network electrode with a large nanowire diameter offers a better operational stability, showing opposite trend to that of the untreated electrodes. To demonstrate the potential application of the highly stable silver nano-network, the combination of silver nano-network electrode and SiO_2 NPs has been introduced to address the electrical shorting issue in OSC. Experimental results reveal that the OSCs fabricated on the Ag nano-network:SiO_2 NPs composite electrodes have achieved comparable PCE to the device on commercial ITO substrate. Consequently, the strategy proposed in this paper, aimed to form silver nano-network with improved operational stability, would benefit for the development of low-cost and solution-processed flexible optoelectronic devices.

4. Experimental Section

Highly Stable Ag Nano-Network Electrode Preparation and Stability Characterization: Silver nanowires with different diameters were synthesized according to previous reports.[11,18] Before spin-coating the silver nanowires on glass substrate, the as-prepared silver nanowires were washed by acetone and ethanol for three times and further dispersed in ethanol for achieving proper concentration. For the preparation of the precursor, proper amount of nitric acid was added to the silver nitrate solution (1.5×10^{-3} M) in ethanol to obtain a PH value of about 3, followed by the addition of ascorbic acid with final concentration of 1×10^{-3} M. To form a highly stable and conductive silver nano-network electrode, the newly prepared precursor was dropped on the as-formed silver nanowire film for wetting. The redundant precursor was immediately spun or blown off. A small amount of precursor will reside at the cross of silver nanowires, which will trigger the localized chemical reaction of silver ions reduction and silver atoms deposition. Highly stable silver nano-network electrode would thereby form with the crystalline silver solders at the cross regions of nanowires. In order to characterize the electrical stabilities of silver nano-network electrodes before and after chemical treatment, two electrical contacts were formed at the two opposite ends of each sample electrode by using silver paste, and an electrical power density of 0.5 W cm^{-2} was applied between the two electrical contacts. The electrodes from silver nanowires of three

different diameters after the chemical treatment were adjusted to have the same sheet resistance through varying the densities of nanowires on substrate. For the electrodes without chemical treatment, the densities of nanowires were equal to the corresponding treated samples of the same diameters.

Ag Nano-Network:SiO_2 Composite Electrode Preparation: To address roughness issue from highly stable silver nano-network electrodes, especially for the nanowires with large diameter, SiO_2 NPs were adopted here to efficiently fill the voids among nano-networks. The SiO_2 NPs were prepared according to the classic Stöber method. Briefly, 5 mL tetraethyl orthosilicate (TEOS) was dropped into a mixed solution containing 98 mL ethanol, 8 mL distilled water, and 1.6 mL ammonium hydroxide (28%), and allowed stirred for 12 h. The SiO_2 NPs with average diameter of about 50 nm were collected through centrifugation and finally dispersed into 2-methoxyethanol with proper concentration. The Ag nano-network:SiO_2 composite electrode was achieved by dropping the SiO_2 nanoparticle solution on the highly stable silver nano-network electrode and spin-coated at the speed of 3000 rpm s^{-1}. As a reference, TiO_2 nanocrystals with diameter of about 4 nm in ethanol solution had been also adopted to reduce the surface roughness of silver nano-network electrode.

Organic Solar Cells Fabrication: The devices were fabricated on five substrates of Ag nano-network(100 nm):SiO_2, Ag nano-network(60 nm):SiO_2, Ag nano-network(60 nm):TiO_2 composite transparent electrodes and Ag nano-network(100 nm), Ag nano-network(60 nm) electrodes. Briefly, the as-received PEDOT:PSS (Baytron AI 4083) without any modification was spin-coated on the electrodes at the speed of 4000 rpm s^{-1} and allowed to dry on a hotplate of 120 °C for 15 min. The P3HT:$PC_{61}BM$ (1:1, 20 mg mL^{-1} in dichlorobenzene) solution was then spin-coated onto the PEDOT:PSS layer followed by 1 h slow-growth and 130 °C annealing for 10 min. The low-bandgap semiconducting polymer PTB7:$PC_{71}BM$ (1:1.5, 25 mg mL^{-1} in chlorobenzene, with addition of 3% 1,8-di-iodooctane (DIO) in volume concentration) was spin-coated on PEDOT:PSS to form a photoactive layer. Finally, device fabrication was completed by thermal evaporation of Ca (40 nm) and Al (100 nm) as a cathode under vacuum condition. A control device using commercial ITO glass as a bottom transparent electrode had been also fabricated according to the above procedure.

Material and Device Characterizations: Scanning electron microscopy images and transmission electron microscopy images were obtained using Hitachi S-4800 FEG scanning electron microscope and FEI Tecnai G2 20 S-TWIN scanning transmission electron microscope, respectively. The sheet resistances of the electrodes were directly characterized by a standard four-point probe measurement approach, and diffused transmission spectra were obtained from a home-built optics system. Current density–voltage (*J*–*V*) characteristics were measured by using a Keithley 2635 sourcemeter and ABET AM1.5G solar simulator. The work functions of UVO-treated ITO and silver nano-network after chemical treatment were measured by a SKP5050 Scanning Kelvin Probe System (KP Technology Ltd.) with a resolution 1–3 meV. The EQE measurement was performed by a home-built system combining xenon lamp, monochromator, chopper, and a lock-in amplifier together with a calibrated silicon photodetector.

Supporting Information

Supporting Information is available from the Wiley Online Library or from the author.

Acknowledgements

This study was supported by the University Grant Council of the University of Hong Kong (Grant No. 201311159056), the General Research Fund (Grants HKU711813 and HKU711612E), the Collaborative Research Fund (Grant C7045-14E), and RGC-NSFC Grant (N_HKU709/12) from the Research Grants Council of Hong Kong Special Administrative Region, China, and Grant CAS14601 from CAS-Croucher Funding Scheme for Joint Laboratories.

Received: March 13, 2015
Revised: April 30, 2015
Published online: May 27, 2015

[1] K. Ellmer, *Nat. Photonics* **2012**, *6*, 808.
[2] D. S. Hecht, L. B. Hu, G. Irvin, *Adv. Mater.* **2011**, *23*, 1482.
[3] J. F. Salinas, H. L. Yip, C. C. Chueh, C. Z. Li, J. L. Maldonado, A. K. Y. Jen, *Adv. Mater.* **2012**, *24*, 6362.
[4] H. Wu, D. S. Kong, Z. C. Ruan, P. C. Hsu, S. Wang, Z. F. Yu, T. J. Carney, L. B. Hu, S. H. Fan, Y. Cui, *Nat. Nanotechnol.* **2013**, *8*, 421.
[5] S. L. Hellstrom, M. Vosgueritchian, R. M. Stoltenberg, I. Irfan, M. Hammock, Y. B. Wang, C. C. Jia, X. F. Guo, Y. L. Gao, Z. N. Bao, *Nano Lett.* **2012**, *12*, 3574.
[6] X. M. Li, D. Xie, H. Park, T. H. Zeng, K. L. Wang, J. Q. Wei, M. L. Zhong, D. H. Wu, J. Kong, H. W. Zhu, *Adv. Energy Mater.* **2013**, *3*, 1029.
[7] C. C. Chen, L. T. Dou, J. Gao, W. H. Chang, G. Li, Y. Yang, *Energy Environ. Sci.* **2013**, *6*, 2714.
[8] S. R. Ye, A. R. Rathmell, Z. F. Chen, I. E. Stewart, B. J. Wiley, *Adv. Mater.* **2014**, *26*, 6670.
[9] F. Xu, Y. Zhu, *Adv. Mater.* **2012**, *24*, 5117.
[10] J. Y. Lee, S. T. Connor, Y. Cui, P. Peumans, *Nano Lett.* **2008**, *8*, 689.
[11] C. Yang, H. W. Gu, W. Lin, M. M. Yuen, C. P. Wong, M. Y. Xiong, B. Gao, *Adv. Mater.* **2011**, *23*, 3052.
[12] J. Jin, J. Lee, S. Jeong, S. Yang, J. H. Ko, H. G. Im, S. W. Baek, J. Y. Lee, B. S. Bae, *Energy Environ. Sci.* **2013**, *6*, 1811.
[13] L. B. Hu, H. S. Kim, J. Y. Lee, P. Peumans, Y. Cui, *ACS Nano* **2010**, *4*, 2955.
[14] S. De, T. M. Higgins, P. E. Lyons, E. M. Doherty, P. N. Nirmalraj, W. J. Blau, J. J. Boland, J. N. Coleman, *ACS Nano* **2009**, *3*, 1767.
[15] T. Kim, A. Canlier, G. H. Kim, J. Choi, M. Park, S. M. Han, *ACS Appl. Mater. Interfaces* **2013**, *5*, 788.
[16] P. Lee, J. Lee, H. Lee, J. Yeo, S. Hong, K. H. Nam, D. Lee, S. S. Lee, S. H. Ko, *Adv. Mater.* **2012**, *24*, 3326.
[17] S. W. Zhu, Y. Gao, B. Hu, J. Li, J. Su, Z. Y. Fan, J. Zhou, *Nanotechnology* **2013**, *24*, 335202.
[18] H. F. Lu, D. Zhang, X. G. Ren, J. Liu, W. C. H. Choy, *ACS Nano* **2014**, *8*, 10980.
[19] R. Y. Chen, S. R. Das, C. Jeong, M. R. Khan, D. B. Janes, M. A. Alam, *Adv. Funct. Mater.* **2013**, *23*, 5150.
[20] R. Zhu, C. H. Chung, K. C. Cha, W. B. Yang, Y. B. Zheng, H. P. Zhou, T. B. Song, C. C. Chen, P. S. Weiss, G. Li, Y. Yang, *ACS Nano* **2011**, *5*, 9877.
[21] T. Tokuno, M. Nogi, J. Jiu, K. Suganuma, *Nanoscale Res. Lett.* **2012**, *7*, 1.
[22] A. Kim, Y. Won, K. Woo, C. H. Kim, J. Moon, *ACS Nano* **2013**, *7*, 1081.
[23] K. Zilberberg, F. Gasse, R. Pagui, A. Polywka, A. Behrendt, S. Trost, R. Heiderhoff, P. Gorrn, T. Riedl, *Adv. Funct. Mater.* **2014**, *24*, 1 671.
[24] C. C. Chen, L. T. Dou, R. Zhu, C. H. Chung, T. B. Song, Y. B. Zheng, S. Hawks, G. Li, P. S. Weiss, Y. Yang, *ACS Nano* **2012**, *6*, 7185.
[25] J. Lee, P. Lee, H. B. Lee, S. Hong, I. Lee, J. Yeo, S. S. Lee, T. S. Kim, D. Lee, S. H. Ko, *Adv. Funct. Mater.* **2013**, *23*, 4171.
[26] M. S. Lee, K. Lee, S. Y. Kim, H. Lee, J. Park, K. H. Choi, H. K. Kim, D. G. Kim, D. Y. Lee, S. Nam, J. U. Park, *Nano Lett.* **2013**, *13*, 2814.
[27] J. J. Liang, L. Li, K. Tong, Z. Ren, W. Hu, X. F. Niu, Y. S. Chen, Q. B. Pei, *ACS Nano* **2014**, *8*, 1590.

[28] J. S. Woo, J. T. Han, S. Jung, J. I. Jang, H. Y. Kim, H. J. Jeong, S. Y. Jeong, K. J. Baeg, G. W. Lee, *Sci. Rep.* **2014**, *4*, 4804.
[29] E. C. Garnett, W. S. Cai, J. J. Cha, F. Mahmood, S. T. Connor, M. G. Christoforo, Y. Cui, M. D. McGehee, M. L. Brongersma, *Nat. Mater.* **2012**, *11*, 241.
[30] P. N. Nirmalraj, A. T. Bellew, A. P. Bell, J. A. Fairfield, E. K. McCarthy, C. O'Kelly, L. F. C. Pereira, S. Sorel, D. Morosan, J. N. Coleman, M. S. Ferreira, J. J. Boland, *Nano Lett.* **2012**, *12*, 5966.
[31] B. Hwang, H. A. S. Shin, T. Kim, Y. C. Joo, S. M. Han, *Small* **2014**, *10*, 3397.
[32] T. C. Hauger, S. M. I. Al-Rafia, J. M. Buriak, *ACS Appl. Mater. Interfaces* **2013**, *5*, 12663.
[33] J. A. Fairfield, C. Ritter, A. T. Bellew, E. K. McCarthy, M. S. Ferreira, J. J. Boland, *ACS Nano* **2014**, *8*, 9542.
[34] T. B. Song, Y. Chen, C. H. Chung, Y. Yang, B. Bob, H. S. Duan, G. Li, K. N. Tu, Y. Huang, Y. Yang, *ACS Nano* **2014**, *8*, 2804.
[35] S. Han, S. Hong, J. Ham, J. Yeo, J. Lee, B. Kang, P. Lee, J. Kwon, S. S. Lee, M. Y. Yang, S. H. Ko, *Adv. Mater.* **2014**, *26*, 5808.
[36] L. Y. Lu, L. P. Yu, *Adv. Mater.* **2014**, *26*, 4413.
[37] Z. C. He, C. M. Zhong, S. J. Su, M. Xu, H. B. Wu, Y. Cao, *Nat. Photonics* **2012**, *6*, 591.
[38] C. Gu, Y. C. Chen, Z. B. Zhang, S. F. Xue, S. H. Sun, C. M. Zhong, H. H. Zhang, Y. Lv, F. H. Li, F. Huang, Y. G. Ma, *Adv. Energy Mater.* **2014**, *4*, 1301771.
[39] P. Cheng, Y. F. Li, X. W. Zhan, *Energy Environ. Sci.* **2014**, *7*, 2005.
[40] S. J. Liu, K. Zhang, J. M. Lu, J. Zhang, H. L. Yip, F. Huang, Y. Cao, *J. Am. Chem. Soc.* **2013**, *135*, 15326.
[41] G. J. Zhao, Y. J. He, Y. F. Li, *Adv. Mater.* **2010**, *22*, 4355.
[42] Y. H. Liu, J. B. Zhao, Z. K. Li, C. Mu, W. Ma, H. W. Hu, K. Jiang, H. R. Lin, H. Ade, H. Yan, *Nat. Commun.* **2014**, *5*, 5293.
[43] J. R. Tumbleston, B. A. Collins, L. Q. Yang, A. C. Stuart, E. Gann, W. Ma, W. You, H. Ade, *Nat. Photonics* **2014**, *8*, 385.
[44] Q. Q. Gan, F. J. Bartoli, Z. H. Kafafi, *Adv. Mater.* **2013**, *25*, 2385.
[45] T. B. Yang, M. Wang, Y. Cao, F. Huang, L. Huang, J. B. Peng, X. Gong, S. Z. D. Cheng, Y. Cao, *Adv. Energy Mater.* **2012**, *2*, 523.
[46] J. Gao, W. Chen, L. T. Dou, C. C. Chen, W. H. Chang, Y. S. Liu, G. Li, Y. Yang, *Adv. Mater.* **2014**, *26*, 3142.
[47] M. Song, D. S. You, K. Lim, S. Park, S. Jung, C. S. Kim, D. H. Kim, D. G. Kim, J. K. Kim, J. Park, Y. C. Kang, J. Heo, S. H. Jin, J. H. Park, J. W. Kang, *Adv. Funct. Mater.* **2013**, *23*, 4177.
[48] A. Kim, Y. Won, K. Woo, S. Jeong, J. Moon, *Adv. Funct. Mater.* **2014**, *24*, 2462.
[49] J. Krantz, M. Richter, S. Spallek, E. Spiecker, C. J. Brabec, *Adv. Funct. Mater.* **2011**, *21*, 4784.
[50] D. S. Leem, A. Edwards, M. Faist, J. Nelson, D. D. C. Bradley, J. C. de Mello, *Adv. Mater.* **2011**, *23*, 4371.
[51] F. Guo, X. D. Zhu, K. Forberich, J. Krantz, T. Stubhan, M. Salinas, M. Halik, S. Spallek, B. Butz, E. Spiecker, T. Ameri, N. Li, P. Kubis, D. M. Guldi, G. J. Matt, C. J. Brabec, *Adv. Energy Mater.* **2013**, *3*, 1062.
[52] J. H. Yim, S. Y. Joe, C. Pang, K. M. Lee, H. Jeong, J. Y. Park, Y. H. Ahn, J. C. de Mello, S. Lee, *ACS Nano* **2014**, *8*, 2857.
[53] X. Y. Zeng, Q. K. Zhang, R. M. Yu, C. Z. Lu, *Adv. Mater.* **2010**, *22*, 4484.
[54] J. J. Liang, L. Li, X. F. Niu, Z. B. Yu, Q. B. Pei, *Nat. Photonics* **2013**, *7*, 817.
[55] W. Gaynor, G. F. Burkhard, M. D. McGehee, P. Peumans, *Adv. Mater.* **2011**, *23*, 2905.
[56] C. Lofton, W. Sigmund, *Adv. Funct. Mater.* **2005**, *15*, 1197.
[57] Y. N. Xia, Y. J. Xiong, B. Lim, S. E. Skrabalak, *Angew. Chem. Int. Ed.* **2009**, *48*, 60.
[58] H. H. Khaligh, I. A. Goldthorpe, *Nanoscale Res. Lett.* **2013**, *8*, 235